Landscape Ecol (2020) 35:373–388
https://doi.org/10.1007/s10980-019-00951-3

RESEARCH ARTICLE

Snowmelt timing impacts on growing season phenology in the northern range of Yellowstone National Park estimated from MODIS satellite data

Christopher Potter

Received: 12 August 2019 / Accepted: 3 December 2019 / Published online: 3 January 2020

Abstract
Context Trends and geographic patterns of change in vegetation phenology metrics and snowmelt timing from the MODerate resolution Imaging Spectroradiometer (MODIS) satellite data sets were analyzed for the Northern Range of Yellowstone National Park over the period 2001 to 2017.
Objectives The main question posed in this analysis was "Where has the growing season length, amplitude, and integrated greenness cover changed over the past two decades on the Northern Range, particularly in relation to vegetation cover types and the timing of spring snowmelt?"
Methods Phenology metric patterns derived from the Normalized Difference Vegetation Index (NDVI) time-series at 250-m resolution were used to track changes in the growing season length, amplitude, and integrated greenness cover over the past two decades.
Results Trend analysis showed that end of the growing season timing (EOST) and integrated greenness increased significantly over nearly 30% of the Northern Range study area, and NDVI amplitude increased significantly in several large drainages, particularly in shrub-grassland cover types. Significant variation in the start of the growing season (SOST), NDVI amplitude and integrated greenness could be further explained by the timing of spring snow melt. In years with relatively late snowmelt dates (after mid-May), higher plant growth was observed over the ensuing growing season, as captured in the amplitude and integrated greenness metrics, potentially due to elevated snow water inputs that can maintain available soil moisture levels for plant growth into the mid- and late-summer months.
Conclusions The ecological implications of an extended period in November–December when grassland and shrub biomass supplies remain relatively snow-free and readily accessible to grazing ungulates will require further assessments.

Keywords Yellowstone · Northern range · MODIS · NDVI · Start of the growing season · Snow-free date

C. Potter (✉)
NASA Ames Research Center, Moffett Field, CA 94035, USA
e-mail: chris.potter@nasa.gov

Introduction

The Northern (winter) Range of Yellowstone National Park (YNP) is a mosaic of sagebrush-steppe, grassland, and forested plant communities (NRC 2002). The big sagebrush-Idaho fescue dominated areas of this ecosystem are heavily grazed in winters by wild ungulates, and account for slightly more than half of all the non-forested vegetation on the Northern Range (Houston 1982). Bison from the large northern herd of

YNP congregate in the Lamar Valley and on adjacent high-elevation meadows to the south for the summer breeding season, but then migrate in the winter to the northwestern portions of the Northern Range, towards lower-elevation areas around Gardiner, Montana (Plumb et al. 2009). Over the past 30 years, Yellowstone bison have increasingly migrated outside the YNP boundary, with the numbers of animals leaving a function of the changes in winter forage availability due to snow water equivalent (Geremia et al. 2011). Presently, successful long-term conservation of Yellowstone bison will depend on facilitating their migration to these lower-elevation winter ranges in and adjacent to the park (Plumb et al. 2009).

Other important changes in vegetation cover are occurring on the Northern Range as well. Stands of quaking aspen (*Populus tremuloides*) were reported to decline in the late twentieth Century, as mature stands died but were not replaced by young trees (Romme et al. 1995; NRC 2002). The loss of aspens has been linked to heavy herbivory by elk (*Cervus elaphus*) during the winter months, which may have suppressed the growth of young trees (Kauffman et al. 2010). Since the reintroduction of wolves (*Canis lupus*) in the mid-1990s, Painter et al. (2016) reported that many aspen stands on the Northern Range are in the early stages of recovery, owing to increased predation on elk and decreased browsing on young trees.

Climate has changed notably in YNP over the past 30 years. Annual average temperature has increased by nearly 1 °C in Yellowstone since the 1988 fires, and this warming may be affecting the phenology of vegetation (Hansen et al. 2016; Notaro et al. 2019). Potter (2019) reported that climate stations records from YNP indicate that 2005 and 2015 were the warmest years in the past two decades, whereas 2004–2005 and 2009–2010 were the driest overall. Nonetheless, Notaro et al. (2019) reported that areas on YNP which were unburned by the 1988 fires have showed no apparent sign of warming-induced greening, possibility due to the mitigating impacts of periodic droughts.

Satellite image analysis can be an effective method to monitor vegetation greening or browning phenology at local to regional scales (Amiro et al. 2000; Goetz et al. 2005, 2006; Cuevas-Gonzalez et al. 2009; Casady and Marsh 2010; Li and Potter, 2012; Potter 2016). Notably, Potter (2015) analyzed more than 20 years of Landsat 30-m NDVI for the YNP area and concluded that the detectable changes in ecosystem green cover since the wildfires of 1988 have been strongly dependent on periodic variations in annual snowpack water content. Using structural change time series analysis of satellite 250-m resolution NDVI data for YNP, Potter (2019) reported that years with relatively high water content in the snowpack, such as 2007–2008 and 2010–2011, were closely associated with abrupt negative shifts in NDVI. This finding implied that snowmelt timing can be a major control over vegetation growth and phenology on the Northern Range.

Remote sensing of land-surface phenology can also be used characterize vegetation changes from one growing season to the next, and to map out specific phenological events, such as start and end of season timing (SOST and EOST) each year (Meier et al. 2015). Potter and Brooks (1998) were among the first to show that such phenological events, as captured by global satellite NDVI data, can be accurately predicted from inter-annual climate variations. This study documented that (1) the annual precipitation total and annual moisture index together can account for 70–80% of the geographical variation in the NDVI seasonal extremes (maximum and minimum values, Fig. 1) and (2) the rate of increase or decrease in NDVI with respect to its annual maximum level was a function of annual temperatures, specifically that a shorter growing season was observed in colder temperatures regions. Ji and Peters (2004) confirmed that precipitation and potential evapotranspiration

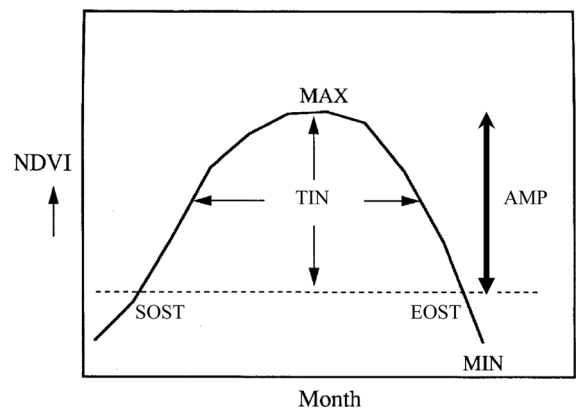

Fig. 1 Hypothetical annual phenology profile based on satellite NDVI time series (after Potter and Genovese 1996), showing the Start of season timing (SOST), End of season timing (EOST), Total integrated NDVI (TIN), Growing season NDVI amplitude (AMP)

were the most significant climatic variables to predict NDVI phenological patterns for grasslands of the Great Plains (USA).

The specific objective of this study was to understand the patterns of change in vegetation phenology metrics and snowmelt timing on the Northern Range of YNP since the year 2000 by combining MODIS NDVI and snow cover data sets. The overarching question posed in this analysis was "Where has the growing season length, amplitude, and integrated greenness cover changed over the past two decades on the Northern Range, particularly in relation to vegetation cover types and the timing of spring snowmelt?" Statistical analysis of change in the MODIS NDVI time series was more closely examined for selected locations using the "Breaks for Additive Seasonal and Trend" method (BFAST, Verbesselt et al. 2010a, b; Potter 2019). The general ecological topic being addressed in this study was how changes in the length of grassland and shrub growing seasons (with relatively snow-free conditions) may affect the forage accessible to grazing ungulates.

Study area

YNP covers 8980 km^2 and extends from elevations of 1540 m to 3760 m (NW corner coordinates: 45° 15′ N, 111° 12′ W; SE corner coordinates: 44° 5′ N, 109° 49′ W, Fig. 2). The montane forest zone in YNP is found between 1200 and 1800 m, and the subapline forest zone is located between 1800 and 2700 m, approaching timberline (Habeck 1987).

The forests of YNP consist of five main conifer species (Kokaly et al. 2003), namely lodgepole pine (*Pinus contorta*), whitebark pine (*Pinus albicaulis*), Douglas fir (*Pseudotsuga menziesii*), Engelmann spruce (*Picea engelmannii*), and subalpine fir (*Abies lasiocarpa*). The wildfires of 1988 burned over 2500 km^2 in YNP and surrounding lands, and created a mosaic of burn severity classes, including light surface burn, severe surface burn, and crown fire. (Despain 1990, Fig. 2, study area map). Climate warming over recent decades has been associated with earlier spring snowmelt, expanded fire seasons, insect outbreaks and tree mortality (Notaro et al. 2019).

The Northern Range of YNP is a mixed landscape of forests and shrublands dominated by big sagebrush (*Artemisia tridentata* ssp. *vaseyana*) and Idaho fescue

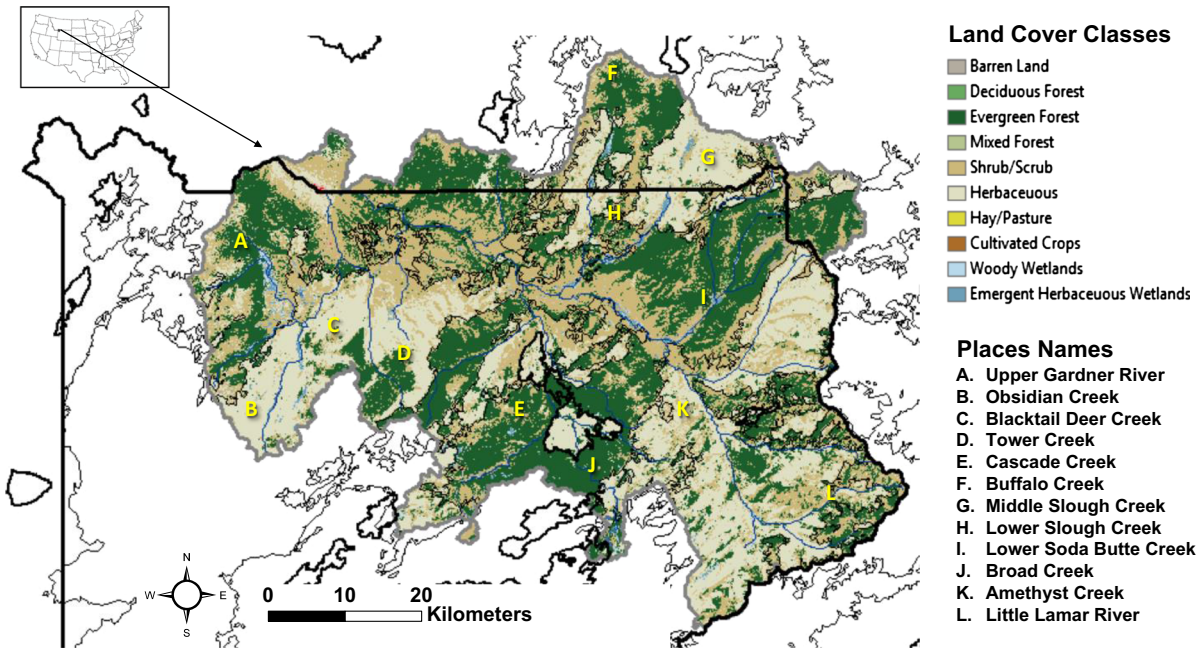

Fig. 2 NLCD map with MTBS fire boundaries (1988, and since 2000 in bold lines) for the Northern Range

(*Festuca idahoensis*). Sagebrush shrub-grasslands are common at elevations of 1800 to 2400 m within the 40- to 75-cm annual precipitation zone (NRC 2002). The Northern Range is drier and warmer than the rest of YNP, with mean snow water equivalents decreasing from 30 to 2 cm along its east–west elevation gradient from Slough Creek to the Gardner River (Plumb et al. 2009). Bison predominantly feed on graminoids, sedges (*Carex* spp.), and rushes (*Juncus* spp.) across the extensive grasslands (Meagher 1973), and share this range with the large Yellowstone elk herd.

Methods

MODIS vegetation index time series

NASA's MODIS (Moderate Resolution Imaging Spectroradiometer) sensors onboard the Terra and Aqua satellites have been used to generate a 250-m resolution NDVI (MOD13) global product on 16-day intervals since the year 2000 (Huete et al. 2002; LP-DACC 2007; Shao et al. 2016). The MODIS Collection six data set offers NDVI vegetation canopy greenness values according to the equation:

$$\mathrm{NDVI} = (\mathrm{NIR} - \mathrm{Red})/(\mathrm{NIR} + \mathrm{Red})$$

where NIR is the reflectance of wavelengths from 0.7 to 1.0 μm and Red is the reflectance from 0.6 to 0.7 μm, with values scaled to between -1.0 and 1.0 NDVI units to preserve decimal places in integer file storage. Low values of NDVI (near 0.1) indicate barren land cover whereas high values of NDVI (above 0.8) indicate dense canopy greenness cover.

The MOD13 250-m vegetation indices (VIs) have been retrieved from daily, atmosphere-corrected, bidirectional surface reflectance (available at modis.gsfc.nasa.gov/data/dataprod/mod13.php). The VIs were computed from MODIS-specific compositing methods based on product quality assurance metrics to remove all low quality pixels from the final NDVI value reported.

The Remote Sensing Phenology (RSP; Meier et al. 2015) program developed by the U.S. Geological Survey (USGS) has produced several phenology metric products (listed Table 1 and also shown in Fig. 1) from MOD13 250-m NDVI data sets that cover all of the continental United States (CONUS) over the years 2001 to 2017. The RSP calculates phenological metrics from time-series NDVI data using a curve derivative method, which employs a backward-looking or delayed moving average (DMA). DMA values are predicted values based on previous observations along a time-series NDVI curve (Reed et al. 1994). Smoothed NDVI data values are compared to a moving average of the previous n observations to identify departures from an established trend. The trend change is defined as the point where the smoothed NDVI values become larger than those predicted by the DMA. This departure point is labeled as the start of the growing season timing metric (SOST). The EOST metric is calculated in a similar manner, with the moving average run in reverse. Once these two parameters are defined, additional metrics are readily derived.

Elevation and land cover map layers

Digital elevation (in vertical meters) was derived from USGS (2016) mapping at 30-m resolution. Drainage basin boundaries and names at the HU10 and HU12 levels for the study area were obtained from the USGS hydrologic unit (HU) database (Seaber et al. 1987). Vegetation cover types were mapped at 30-m resolution from the 2006 National Land Cover Dataset (NLCD, Homer et al. 2015; Fig. 2), available online at www.mrlc.gov.

MODIS snowmelt timing products

Snowmelt timing maps (STMs) for North America were obtained from the database developed by O'Leary et al. (2017), based on the MODIS 8-day composite snow-cover product (MOD10A2) and covering the time period from 2001 to 2018. The MOD10A2 product is derived from the Normalized Difference Snow Index (NDSI) using a 50% snow/no-snow classification threshold. Snowmelt timing (for the first no-snow Julian day of the year) was defined as a snow-free reading following two consecutive snow-present readings for a given 500-m STM pixel. STM products have been validated using in situ observations and comparisons with SNOTEL meteorological stations from across the western United States (NRCS 2016).

Table 1 Phenology metric definitions (from Meier et al. 2015)

Metric	Abbreviation	Definition
Amplitude	AMP	Maximum increase in canopy photosynthetic activity above the growing season baseline (i.e., the minimum seasonal NDVI value)
End of season timing	EOST	End date of measurable photosynthesis in the vegetation canopy
Start of season timing	SOST	Beginning data of measurable photosynthesis in the vegetation canopy
Time-integrated NDVI	TIN	Canopy photosynthetic activity across the entire growing season

Statistical analysis methods

Following the approach of O'Leary et al. (2016) for comparisons of snow-free dates across drainage basins to disturbance areas and numbers, the dates of STM were transformed into relative values by Z-score calculation (Aho 2014) of the number of standard deviations from the mean over all years. A negative Z-score indicated a year with an earlier snowmelt relative to the multi-year mean.

Time series analysis of MOD13 16-day NDVI values over the period 2000 to 2017 was carried out at selected locations using the BFAST methodology developed by Verbesselt et al. (2010a, b), to plot the original NDVI seasonal curves from which the MODIS phenology metrics were derived. This R package was applied by Potter (2019) to all of YNP for detecting and characterizing abrupt changes in green cover, while also adjusting for repeated growing season cycles of NDVI. A harmonic seasonal model is first applied in BFAST to account for regular seasonal phenological variations. BFAST next computes and plots the Ordinary Least Squares Moving Sum (OLS-MOSUM) by considering the moving sums of the residuals after the harmonic seasonal model has been removed from the time series data values. If a "no data" value was present in the growing season MOD13 record, then the NDVI from the previous 16-day period was substituted.

Results

NDVI phenology for vegetation classes

The largest contiguous areas of deciduous forest, coniferous (evergreen) forest, shrubland, grassland, and wetland cover from the 30-m NLCD of the Northern Range area study were identified to summarize and define the characteristic range of NDVI phenology metrics derived by Meier et al. (2015) over the period 2001 to 2017. Results showed that grassland and deciduous forest had the earliest SOST, followed by wetland, shrubland and coniferous forest (Table 2). Coniferous forest and grassland had the latest EOST and deciduous forest had the earliest EOST. Wetland, shrubland and deciduous forest had the highest AMP, whereas grassland had the lowest AMP.

Start and end of season timings

The map for trends in SOST (Fig. 3) from 2001 to 2017 showed that only 3% of all MODIS 250-m resolution pixel locations experienced a significant ($p < 0.05$) increase (i.e., a later) start of the growing season over the period, whereas less than 0.1% experienced a significant ($p < 0.05$) decrease (i.e., an earlier) start of the growing season. Among all of the locations that showed significant increase in the start of the growing season since the year 2001 (starting at a mean date of May 5), equivalent to nearly 4 days later by 2017, 56% were in shrub-grassland cover and 44% in (coniferous) forest cover, mainly in drainages of the Upper Gardner River, Blacktail Deer Creek, and Lower Slough Creek (place names labelled in Fig. 2). The trend regression coefficients (r) ranged from -0.75 to $+0.75$. About 22% of the variability in all r values for SOST was explained by increasing elevation, from 1500 to 3300 m, over the Northern Range, i.e., later SOST trends were more common at higher elevation locations.

The linear (least squared regression) correlation of the yearly SOST date of NDVI phenology with the MODIS snow-free date in the springtime for that year showed a map (Fig. 4a) with 7% of the study area having a significant ($p < 0.05$) positive relationship between these two variables. The drainages with the

Table 2 Characteristic NDVI phenology metrics derived for NLCD vegetation classes on the Northern Range

Vegetation Class	NLCD Code	Number of pixels	SOST median (DOY)	SOST majority (DOY)	EOST median (DOY)	EOST Majority (DOY)	AMP median	AMP majority
Deciduous forest	41	10	121	111	306	306	52	52
Coniferous forest	42	3512	138	141	328	339	40	33
Shrubland	52	7007	143	148	304	290	54	53
Grassland	71	166	93	92	326	326	25	25
Wetland	95	38	128	128	321	319	70	71

Units are in day of year (DOY) or NDVI summation for AMP

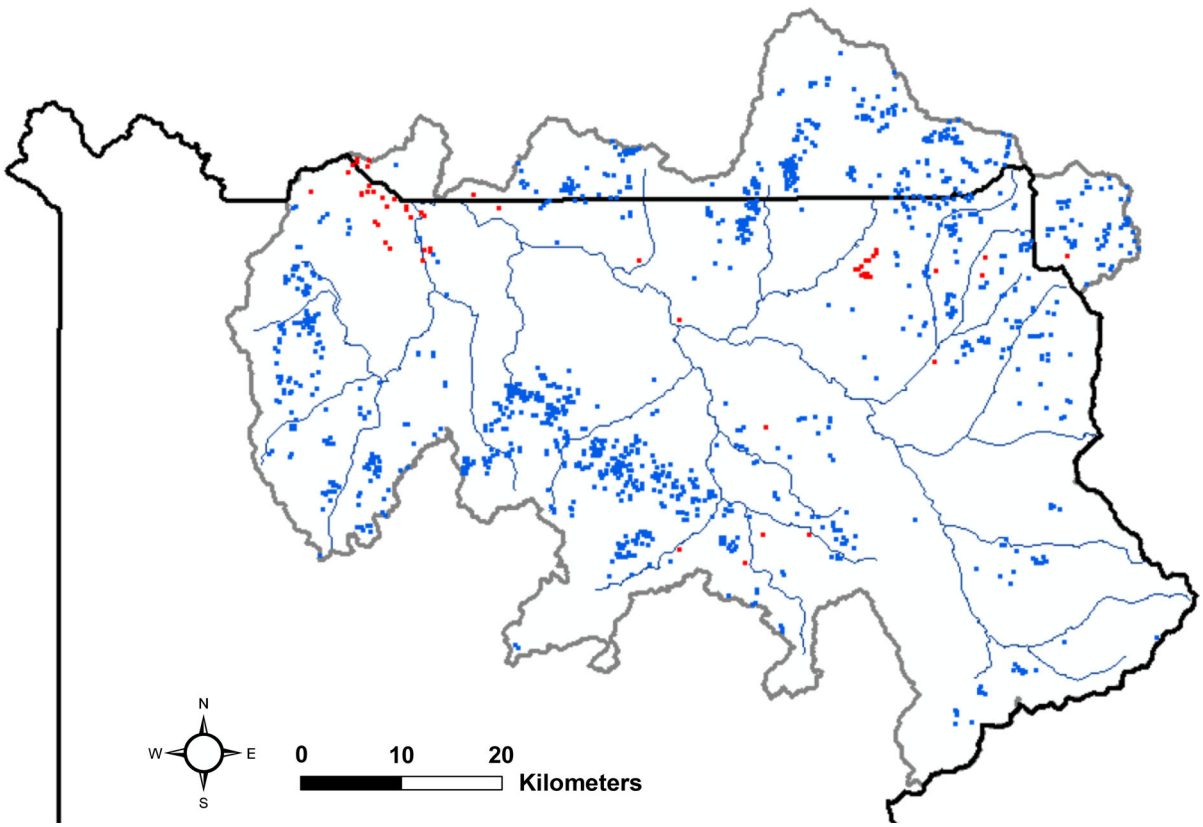

Fig. 3 Trend over the years 2001 to 2017 in the Start of Season Timing (SOST) in MODIS NDVI. Significance levels at $p < 0.05$ for $r < -0.5$ (Red) or $r > +0.5$ (Blue). (Color figure online)

highest concentration of locations of significant later SOST date correlations with later snowmelt timing were Blacktail Deer Creek, Buffalo Creek, Lower Slough Creek, and Amethyst Creek. Averaged across the Northern Range study area (Fig. 4b), 2008 and 2011 were the years with the latest snow-free dates (after June 10), whereas 2015 was the years with the earliest snow-free dates (before May 8).

The trend map for EOST (Fig. 5) showed that 28% of all MODIS 250-m resolution pixel locations experienced a significant ($p < 0.05$) increase (i.e., a later) end of the growing season over the period 2001 to 2017, whereas less than 0.1% experienced a significant ($p < 0.05$) decrease (i.e., an earlier) end of the growing season. The average increase over the study area in the end of the growing season since the year 2001 (starting at a mean date of Nov 10) was

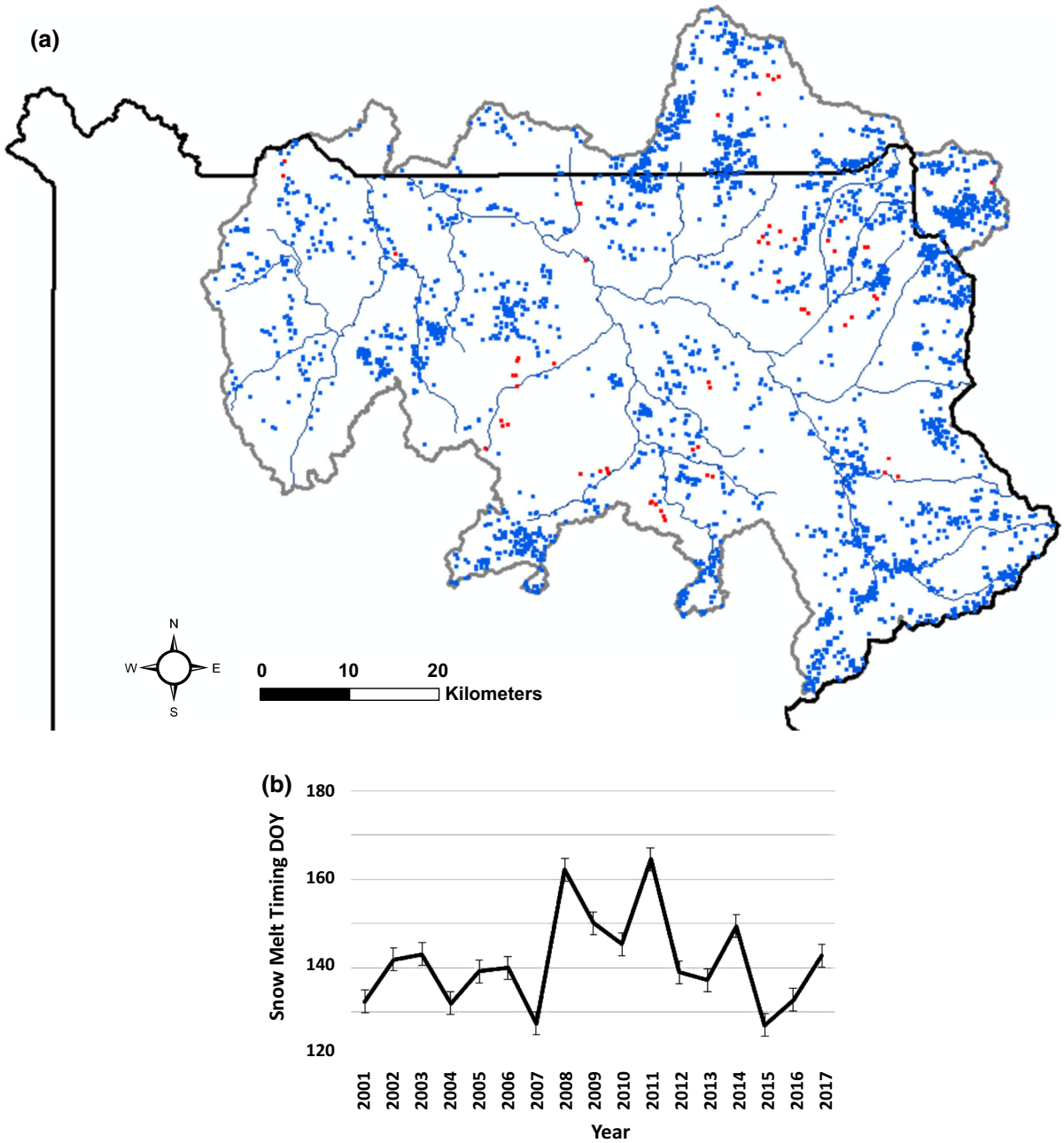

Fig. 4 **a** Correlation over the years 2001 to 2017 between Snowmelt Timing (STM) and Start of Season Timing (SOST) in MODIS NDVI. Significance levels at $p < 0.05$ for $r < -0.5$ (Red) or $r > +0.5$ (Blue). **b** Time series plot of average snowmelt timing day of the year for the study area. Error bars represent one standard error of the mean. (Color figure online)

16 days later by 2016–2017. About 71% of the locations that showed significant later EOST trend were in shrub-grassland cover and 29% in forest cover, distributed across all major drainages of the study area. Significant variations in the trend regression coefficients (r) for EOST were not explained by elevation, nor by association with snowmelt timing dates of the years 2001 to 2017.

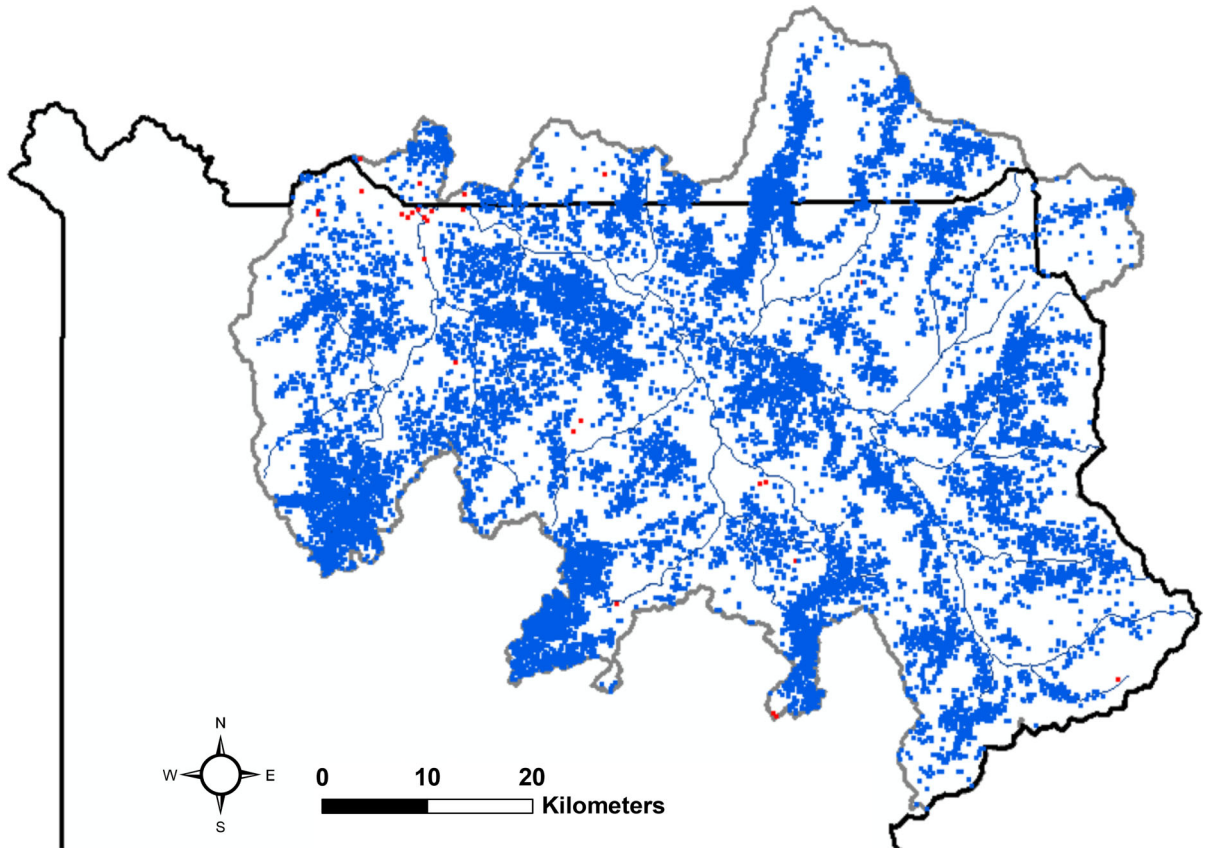

Fig. 5 Trend over the years 2001 to 2017 in the End of Season Timing (EOST) of MODIS NDVI. Significance levels at $p < 0.05$ for $r < -0.5$ (Red) or $r > +0.5$ (Blue). (Color figure online)

Growing season NDVI amplitude

The trend map for the AMP of growing season NDVI (Fig. 6) showed that 4% of all MODIS 250-m resolution pixel locations experienced a significant ($p < 0.05$) increase in the growing season amplitude over the period 2001 to 2017, whereas 4.5% experienced a significant ($p < 0.05$) decrease in the growing season amplitude. About 58% of the locations that showed significant increase in AMP since the year 2001 were in shrub-grassland cover and 42% in forest cover, mainly in drainages of Cascade Creek and Lower Soda Butte Creek (place names labelled in Fig. 2). About 85% of the locations that showed significant decrease in AMP since the year 2001 were in shrub-grassland cover and 15% in forest cover, mainly in drainages of Obsidian Creek, Blacktail Deer Creek, Lower Slough Butte Creek, and Broad Creek.

Significant variations in the trend regression coefficients (r) for AMP were not explained by elevation. However, the linear (least squared regression) correlation of the yearly AMP of NDVI phenology with the MODIS snow-free date in the springtime for that year showed a map (Fig. 7) with 18% of the study area having a significant ($p < 0.05$) positive relationship between these two variables. The drainages with the highest concentration of locations of significantly higher AMP with later snowmelt timing were the Upper Gardner River, Tower Creek, Buffalo Creek, Middle and Lower Slough Creek, Lower Soda Butte Creek, and Broad Creek.

Growing season integrated NDVI

The trend map for growing season TIN (Fig. 8) showed that 5% of all MODIS 250-m resolution pixel locations experienced a significant ($p < 0.05$) increase in TIN over the period 2001 to 2017, whereas 3% experienced a significant ($p < 0.05$) decrease in TIN. About 77% of the locations that showed significant

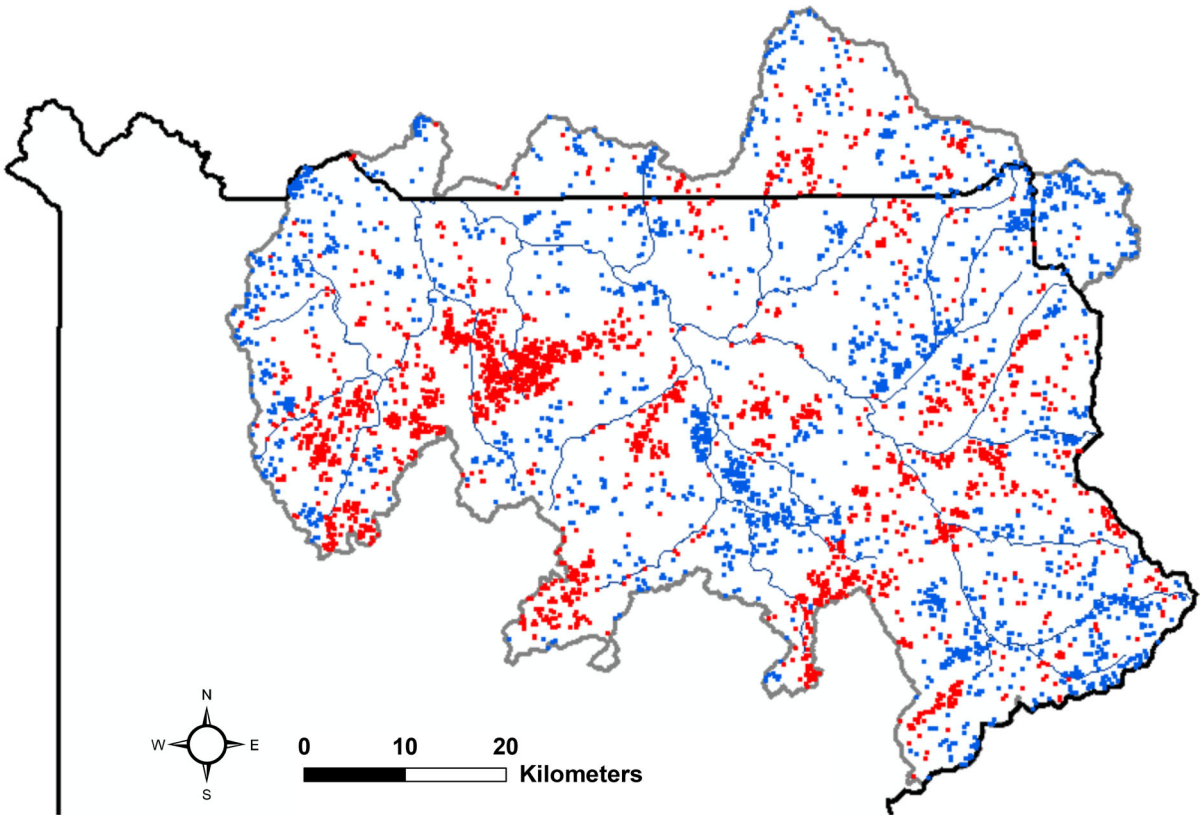

Fig. 6 Trend over the years 2001 to 2017 in the growing season amplitude (AMP) of MODIS NDVI. Significance levels at $p < 0.05$ for $r < -0.5$ (Red) or $r > +0.5$ (Blue). (Color figure online)

increase in TIN since the year 2001 were in shrub-grassland cover and 23% in forest cover, mainly in drainages of Broad Creek and Middle Slough Creek. About 88% of the locations that showed significant decrease in TIN since the year 2001 were in shrub-grassland cover and 12% in forest cover, mainly in drainages of Obsidian Creek, Blacktail Deer Creek, and Middle Slough Creek. Significant variations in the trend regression coefficients (r) for TIN were not explained by elevation.

Nonetheless, the linear (least squared regression) correlation of the yearly TIN of NDVI phenology with the MODIS snow-free date in the springtime for that year showed a map (Fig. 9) with 16% of the study area having a significant ($p < 0.05$) positive relationship between these two variables. The drainages with the highest concentration of locations of significantly higher TIN with later snowmelt timing were the Upper Gardner River, Blacktail Deer Creek, Tower Creek, Buffalo Creek, Middle and Lower Slough Creek, Lower Soda Butte Creek, and Little Lamar River. Moreover, 30% of the variability in all r values for TIN was explained by elevations from 1500 to 3400 m over the Northern Range, i.e., increasing TIN trends with late snowmelt dates were more common at lower elevation locations. An example time series of growing season TIN (and the EOST) for grassland sites located near 2300 m elevation in the Buffalo Creek drainage of the study area (Fig. 10) showed that the increase started after the relatively dry years in YNP of 2001 to 2004 (Potter 2019) and was maintained from 2009 to 2017, with the exception of the extreme early snowmelt year of 2015.

To more closely examine changes in NDVI for selected locations on the Northern Range that showed significantly ($p < 0.05$) increasing EOST and TIN phenology trends, BFAST time series plot outputs of MOD13 NDVI values were generated for four different locations of interest (Fig. 11). The full 16-day NDVI time series (top *Yt* panel) for each location and the fitted trend component (middle *Tt* panel) indicated a slope of increasing green cover, particularly after

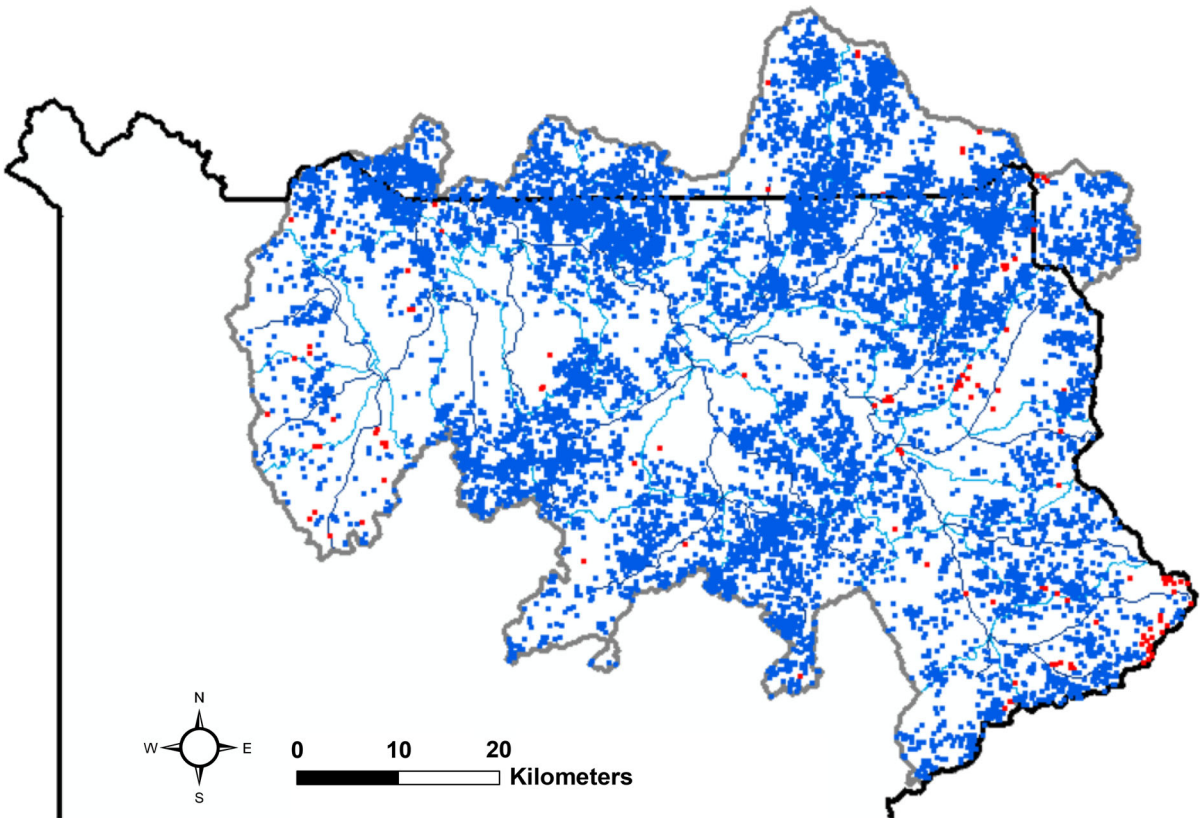

Fig. 7 Correlation over the years 2001 to 2017 between Snowmelt Timing (STM) and the growing season amplitude (AMP) of MODIS NDVI. Significance levels at $p < 0.05$ for $r < -0.5$ (Red) or $r > +0.5$ (Blue). (Color figure online)

2009, at all locations. For the Gardner River basin grassland examples (Figs. 11a, b), the end-of-growing season minimum NDVI period between the yearly growing season profiles were notably longer over the period 2015–2017 than in the previous 15 years. Additionally, the annual TIN from shrub-grassland locations in the Buffalo Creek and Middle Slough Creek drainages (Figs. 11c, d) showed steadily increasing green cover trends that were not negatively impacted by the relatively late snowmelt in the years 2008 and 2011, nor by the extreme early snowmelt pattern in 2015.

Discussion

Results from this time series analysis of NDVI phenology metrics developed by the USGS (RSP; Meier et al. 2015) showed that growing season length, amplitude, and integrated greenness cover have all increased significantly in several large drainages on the Northern Range of YNP over the past two decades, particularly in shrub-grassland cover types. Significant variation in the shifts for SOST, NDVI amplitude and integrated greenness could be further explained by the timing of spring snow melt over the time period of 2001 to 2017. The drainages that had the greatest area coverage of significantly later SOST and higher AMP and TIN together with periodically later snowmelt timing were the Upper Gardner River, Blacktail Deer Creek, Tower Creek, Buffalo Creek, Middle and Lower Slough Creek, Lower Soda Butte Creek, Amethyst Creek, and Broad Creek.

Using MODIS 250-m NDVI data from the years 2000 to 2018 in time series breakpoint (disturbance) analysis, Potter (2019) documented numerous areas across the Northern Range of YNP with a relatively high frequency of abrupt negative shifts in NDVI and relatively high snowpack and snow water equivalent (SWE) levels in concurrent seasons, particularly over

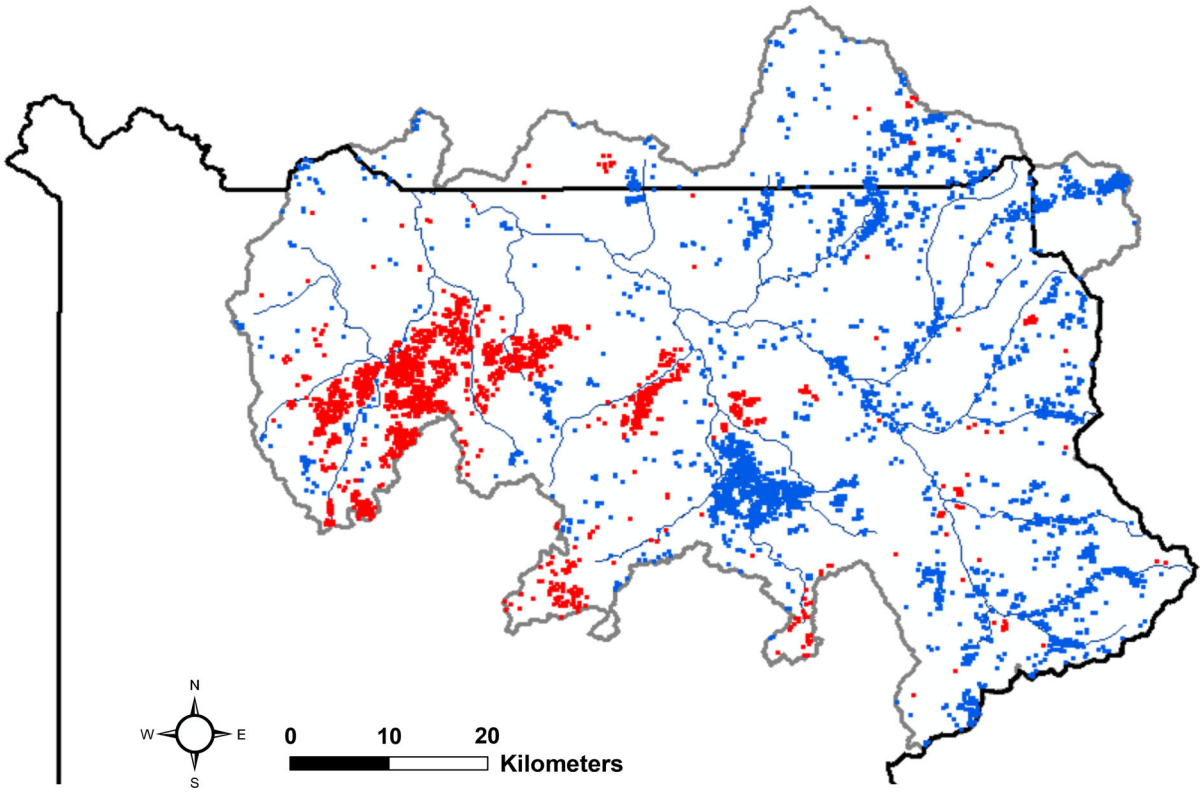

Fig. 8 Trend over the years 2001 to 2017 in the growing season Time Integrated NDVI (TIN). Significance levels at $p < 0.05$ for $r < -0.5$ (Red) or $r > +0.5$ (Blue). (Color figure online)

the periods 2007–2008 and 2010–2011. In addition, Potter (2015) determined from Landsat image analysis (for unburned ecosystems of YNP), that unprecedented periodic decline in SWE over the years 1985 to 2005 had significant negative impacts on green vegetation cover. These results together support the hypothesis that, in years with relatively late snowmelt dates (after mid-May), there can be a delay the green-up of vegetation on the Northern Range, but that higher plant growth over the ensuing growing season, as captured in the AMP and TIN metrics, will be augmented by elevated SWE from the springtime melt maintaining available soil moisture levels into the mid-to late-summer months.

Although there remains limited evidence to link spring snowmelt timing to the widespread persistence of soil water availability during warm summer months, Blankinship et al. (2014) addressed this topic by manipulating the timing of seasonal snowmelt in a high-elevation mixed-conifer forest in the Sierra Nevada during consecutive wet and dry years. Their results showed that shallow soil water layers (0–30 cm depth) responded strongly to snowmelt timing. The influence of delayed snowmelt lasted for 2 months in the 0–15 cm soil layer and at least 4 months in the 15–30 cm soil layer. It was concluded that the legacy of snowmelt timing on soil moisture can persist through late-summer dry periods in western U. S. mountain watersheds. If snowmelt occurs after plant evaporative demand increases, then the shallow soil layers can capture more of the slowly melting water. Conversely, earlier water transfer from the melting snowpack into the soil can induce a water deficit that persists throughout the growing season.

Increased green vegetation cover (captured by the TIN metric) in summer and fall seasons following relatively late snowmelt timing was evident all along the northern boundary of YNP (Fig. 9). These patterns were detected extensively in sagebrush-grassland corridors of the Gardner River, Buffalo Creek, and Middle Slough Creek basis, where ungulates would trend to migrate out of the national park protected area

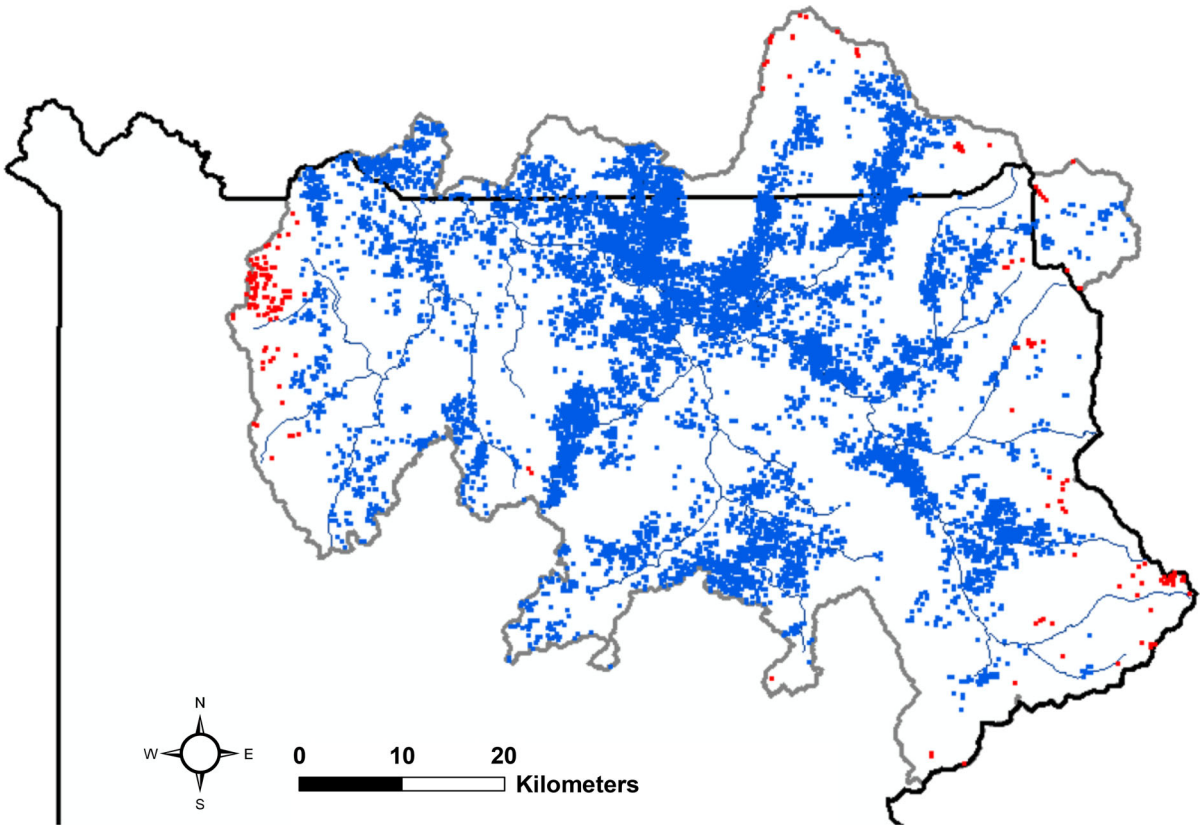

Fig. 9 Correlation over the years 2001 to 2017 between Snowmelt Timing (STM) and the growing season Time Integrated NDVI (TIN). Significance levels at $p < 0.05$ for $r < -0.5$ (Red) or $r > +0.5$ (Blue). (Color figure online)

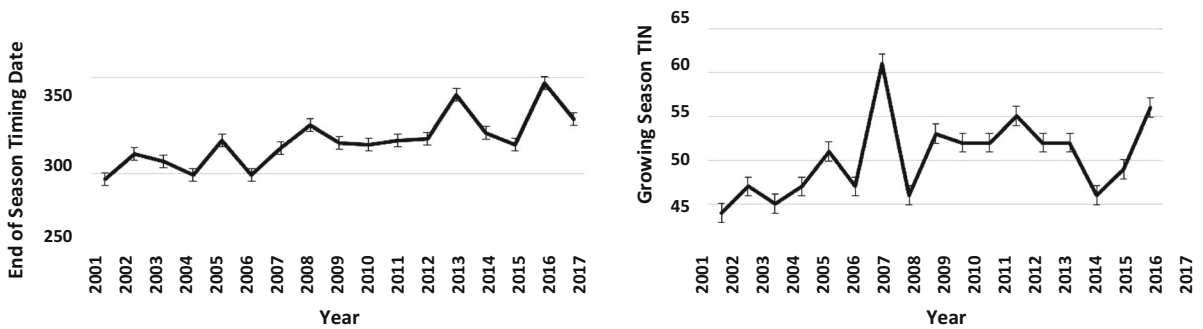

Fig. 10 Example time series of EOST and growing season TIN for grassland sites in the Buffalo Creek drainage of the study area. Error bars represent one standard error of the mean

(Geremia et al. 2011). In years when snowmelt timing has been unusually early, such as 2015, the growing season ended earlier in these areas and the TIN metric declined to its lowest level in many years.

The significant trend patterns of declining AMP and TIN levels from 2000 to 2017 in the drainages from Obsidian Creek to Blacktail Deer Creek and also in the Tower Creek and Cascade Creek drainages (Figs. 6, 8) occurred in major grasslands ecosystems of the Northern Range, which were not burned by wildfires in 1988 or more recently. These declines in growing season NDVI accelerated notably after 2015 and could have been driven by the extreme early snowmelt

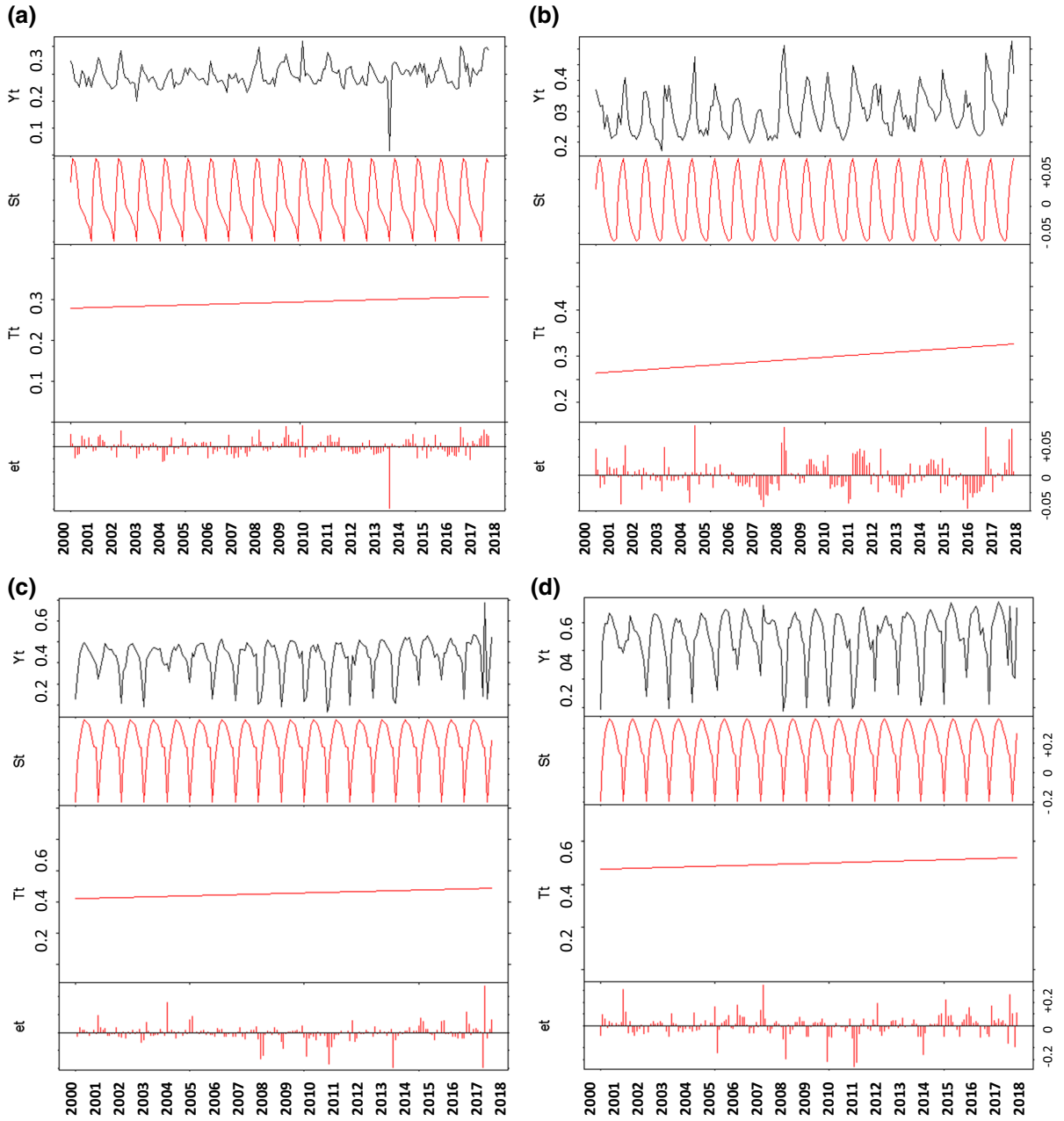

Fig. 11 BFAST output plots (2000 to 2018) of 250-m MODIS NDVI for selected locations on the Northern Range (labelled in Fig. 2) that showed significantly ($p < 0.05$) increasing EOST and TIN phenology trends. Selected locations were grassland sites in the Gardner River drainage (**a** 45.05101° N, − 110.7269° W) and (**b** 45.0573° N, − 110.7067° W) and shrub-grassland sites in the **c** Buffalo Creek (45.0448° N, − 110.3139° W) and **d** Middle Slough Creek (45.0365° N, − 110.1947° W) drainages. *Yt* is the time-series MODIS NDVI value; *St* is the fitted seasonal component; *Tt* is the fitted trend component; *et* is the residual "noise" component (Verbesselt et al. 2010a)

season of 2015, with an expected soil water deficit during that growing season.

Changes over time in the start and end dates of the growing season in YNP must be explained by somewhat different casual factors. Most of the later SOST trends detected over the Northern Range were more common at relatively high elevation locations. This finding implies that deeper snow packs and

higher SWE levels above 3000 m elevation have been less affected by warming springtime temperatures than in the lowland creek and river bottoms areas. On the other hand, the finding that nearly one-third of the Northern Range has experienced a significant increase (i.e., a later) end of the growing season over the period 2000 to 2017, which was not strongly related to snowmelt timing trends, suggests that late-summer and autumn climate conditions have substantially expanded the snow-free season length in this part of YNP, with a general trend in EOST illustrated in Fig. 10.

The ecological implications of an extended period in November–December when grassland and shrub biomass supplies remain relatively snow-free and readily accessible to grazing ungulates in YNP have yet to be assessed, but may be substantial. Plumb et al. (2009) have written that bison in YNP recently expanded their winter range to lower elevations, both inside and outside the national park, as their numbers increased and climatic factors (i.e., snow, drought) have interacted with density to limit nutritional intake and foraging efficiency. Snow cover is considered the primary factor that reduces foraging efficiency for bison, and as snow depth increases, the available foraging area for Yellowstone bison is reduced to lower elevation areas and on thermally warmed ground. However, since 2009, the Yellowstone bison population has nearly doubled in size (Geremia et al. 2017). The trends toward lower SWE, earlier snowmelt timing, and extended fall snow-free conditions detected (for higher accumulated TIN) from MODIS time series analysis together imply that winters on the Northern Range are becoming more favorable for the bison herd.

Aspen growing on the Northern Range of YNP occurs in small- to medium-sized stands growing on moist areas of the landscape (NRC 2002), most of which are too small to be easily monitored using 250-m resolution MODIS NDVI products. While the upper elevation limits for aspen may be determined by growing season length (Mueggler 1988), and despite the fact that EOST in many drainages on the Northern Range has increased by more than a week since 2000, it does not appear feasible to detect exactly where deciduous tree stands have expanded in the study area from the MODIS time-series analysis. It can only be implied that among the most probable locations for expansion of aspen stands would be in the Cascade Creek, Middle Slough Creek, and Lower Soda Butte Creek drainages, where both EOST and AMP trends have favored deciduous woody vegetation phenology and growth.

According to Kay (2018), repeated heavy browsing has at times affected aspen, willow, and cottonwood communities on the Northern Range, despite a 60% reduction in elk numbers from 2000 to 2018 (Mosley and Mundinger 2018). One potential explanation is that browsing by bison has increased (Painter and Ripple 2012), and has filled some of the void in herbivory created by a reduction in the YNP elk herds. Much of the scattered recovery of deciduous woody vegetation on the Northern Range inside YNP has occurred in isolated locations where bison have not been observed in large numbers (Painter et al. 2014).

Conclusions

Trend analysis for MODIS phenology metrics (2000 to 2017) showed, for the first time, that end of the growing season timing (EOST) and integrated greenness have increased significantly over nearly 30% of the Northern Range of Yellowstone National Park. NDVI amplitude has increased significantly since 2000 in several large drainages, particularly in shrub-grassland cover types. Years with relatively late snowmelt dates (after mid-May) were associated with higher plant growth over the ensuing growing season, possibly due to elevated snow water inputs that can maintain available soil moisture levels for plant growth into the mid- and late-summer months.

Acknowledgements This work was conducted with the support from NASA Ames Research Center. The author thanks Donal O'Leary for providing updated MODIS snowmelt timing maps through 2018.

References

Aho KA (2014) Foundational and applied statistics for biologists. Chapman & Hall, CRC Press, London

Amiro BD, Chen JM, Liu J (2000) Net primary productivity following forest fire for Canadian ecoregions. Can J For Res 30:939–947

Blankinship JC, Meadows MW, Lucas RG, Hart SC (2014) Snowmelt timing alters shallow but not deep soil moisture in the Sierra Nevada. Water Resour Res 50:1448–1456

Casady GM, Marsh SE (2010) Broad-scale environmental conditions responsible for post-fire vegetation dynamics. Remote Sens 2:2643–2664

Cuevas-Gonzalez M, Gerard F, Balzter H, Riano D (2009) Analysing forest recovery after wildfire disturbance in boreal Siberia using remotely sensed vegetation indices. Glob Change Biol 15:561–577

Despain D (1990) Yellowstone vegetation: consequences of environment and history in a natural setting. Roberts Rinehart, Boulder

Geremia C , Wallen R, White PJ (2017) Status Report on the Yellowstone Bison Population, September 2017, Report for the Interagency Bison Management Plan. http://ibmp.info/

Geremia C, White P, Wallen R, Watson F, Treanor J, Borkowski J, Potter C, Crabtree R (2011) Predicting bison migration out of Yellowstone National Park using Bayesian Models. PLoS ONE 6(2):e16848. https://doi.org/10.1371/journal.pone.0016848

Goetz SJ, Bunn AG, Fiske GJ, Houghton RA (2005) Satellite observed photosynthetic trends across boreal North America associated with climate and fire disturbance. Proc Natl Acad Sci 103:13521–13525

Goetz SJ, Fiske GJ, Bunn AG (2006) Using satellite time-series data sets to analyze fire disturbance and forest recovery across Canada. Remote Sens Environ 101:352–365

Hansen WD, Romme WH, Ba A, Turner MG (2016) Shifting ecological filters mediate postfire expansion of seedling aspen (*Populus tremuloides*) in Yellowstone. For Ecol Manag 362:218–230

Homer CG, Dewitz JA, Yang L, Jin S, Danielson P, Xian G, Coulston J, Herold ND, Wickham JD, Megown K (2015) Completion of the 2011 National Land Cover Database for the conterminous United States - Representing a decade of land cover change information. Photogramm Eng Remote Sens 81:345–354

Houston DB (1982) The Northern Yellowstone elk: ecology and management. Macmillan, New York

Huete A, Didan K, Miura T, Rodriquez E, Gao X, Ferreira L (2002) Overview of the radiometric and biophysical performance of the MODIS vegetation indices. Remote Sens Environ 83:195

Ji L, Peters AJ (2004) A spatial regression procedure for evaluating the relationship between AVHRR-NDVI and climate in the northern Great Plains. Int J Remote Sens 25:297–311

Kauffman MJ, Brodie JF, Jules ES (2010) Are wolves saving Yellowstone's aspen? A landscape-level test of a behaviorally mediated trophic cascade. Ecology 91:2742–2755

Kay CE (2018) The condition and trend of aspen, willows, and associated species on the Northern Yellowstone Range. Rangelands 40:202–211

Li S, Potter CS (2012) Vegetation regrowth trends in post forest fire ecosystems across North America from 2000 to 2010. Nat Sci. https://doi.org/10.4236/ns.2012

LP-DACC: NASA Land Processes Distributed Active Archive Center (2007) MODIS/Terra Vegetation Indices Monthly L3 Global 0.05Deg CMG (MOD13C2), Version 005. Sioux Falls, South Dakota: USGS/Earth Resource s Observation and Science (EROS) Center

Meagher M (1973) The bison of Yellowstone National Park. Science monographs 1. National Park Service, Government Printing Office, Washington, DC

Meier G, Brown J, Evelsizer R, Vogelmann J (2015) Phenology and climate relationships in aspen (*Populus tremuloides* Michx.) forest and woodland communities of southwestern Colorado. Ecol Indic 48:189–197

Mosley JC, Mundinger JG (2018) History and status of wild ungulate populations on the Northern Yellowstone Range. Rangelands 40:189–201

Mueggler W (1988) Aspen community types of the intermountain region. Gen. Tech. Rep. INT 250. U.S. Department of Agriculture, U. S. Forest Service, Ogden

National Resaerch Council (NRC) (2002) Ecological dynamics on Yellowstone's Northern range. Committee on Ungulate Management in Yellowstone National Park, National Academy Press, Washington, D.C., p 199

Natural Resources Conservation Service (NRCS) (2016) SNOTEL Data & Products, National Water and Climate Center. http://www.wcc.nrcs.usda.gov/snow/. Accessed May 2018

Notaro M, Emmett K, O'Leary D (2019) Spatio-temporal variability in remotely sensed vegetation greenness across Yellowstone National Park. Remote Sens 11:798

O'Leary D III, Bloom T, Smith J, Zemp C, Medler M (2016) A new method comparing snowmelt timing with annual area burned. Fire Ecol. https://doi.org/10.4996/fireecology.1201041

O'Leary D III, DK Hall, M Medler, R Matthews, A Flower (2017) Snowmelt timing maps derived from MODIS for North America, 2001-2015. ORNL DAAC, Oak Ridge, Tennessee, USA. https://doi.org/10.3334/ORNLDAAC/1504. Accessed May 2019

Painter LE, Beschta RL, Larsen EJ, Ripple WJ (2014) After long-term decline, are aspen recovering in northern Yellowstone? For Ecol Manag 329:108–117

Painter LE, Ripple WJ (2012) Effects of bison on willow and cottonwood in northern Yellowstone National Park. For Ecol Manag 264:150–158

Plumb G, White PJ, Coughenour M, Wallen R (2009) Carrying capacity, migration, and dispersal in Yellowstone bison. Biol Conserv 142:2377–2387

Potter C (2015) Vegetation cover change in Yellowstone National Park detected using Landsat satellite image analysis. J Biodivers Manage Forestry 4:3

Potter CS (2019) Changes in vegetation cover of Yellowstone National Park estimated from MODIS greenness trends, 2000 to 2018. Remote Sens Earth Syst Sci. https://doi.org/10.1007/s41976-019-00019-5

Potter CS, Brooks-Genovese V (1996) Global analysis of empirical relations between annual climate and seasonality of NDVI. Int J Remote Sens 19(15):2921–2948. https://doi.org/10.1080/014311698214352

Potter CS, Brooks V (1998) Global analysis of empirical relations between annual climate and seasonality of NDVI. Int J Remote Sens 19:2921–2948

Reed BC, Brown JF, Vanderzee D, Loveland TR, Merchant JW, Ohlen DO (1994) Measuring phenological variability from satellite imagery. J Veg Sci 5:703–714

Romme WH, Turner MG, Wallace LL, Walker JS (1995) Aspen, elk, and fire in northern Yellowstone Park. Ecology 76:2097–2106

Seaber PR, Kapinos FP, Knapp GL (1987) Hydrologic Unit Maps: U.S. Geological Survey Water-Supply Paper 2294, p 63

Shao Y, Lunetta RS, Wheeler B, Iiames JS, Campbell JB (2016) An evaluation of time-series smoothing algorithms for land-cover classifications using MODIS NDVI multi-temporal data. Remote Sens Environ 174:258–265

Verbesselt J, Hyndman R, Newnham G, Culvenor D (2010a) Detecting trend and seasonal changes in satellite image time series. Remote Sens Environ 114:106–115

Verbesselt J, Hyndman R, Zeileis A, Culvenor D (2010b) Phenological change detection while accounting for abrupt and gradual trends in satellite image time series. Remote Sens Environ 114:2970–2980